J. CHEM. SOC. FARADAY TRANS., 1993, 89(16), 2983–2991

Mechanisms of the Cl-atom-initiated Oxidation of Acetone and Hydroxyacetone in Air

Michael E. Jenkin*
AEA Environment & Energy, Building 551, Harwell Laboratory, Didcot, Oxfordshire, UK OX11 0RA
Richard A. Cox
NERC Marine and Atmospheric Sciences, Polaris House, North Star Avenue, Swindon, UK SN2 1EU
Martin Emrich and Geert K. Moortgat
Air Chemistry Department, Max-Plank-Institut für Chemie, Saarstrasse 23, D-6500 Mainz, Germany

The products of the Cl-atom-initiated oxidation of acetone and hydroxyacetone (CH_3COCH_2OH) in O_2–N_2 mixtures at 700 Torr and 298 K have been identified using long-path-length FTIR spectroscopy and long-path-length UV–visible diode array spectroscopy. The oxidation of acetone yields methyl glyoxal (CH_3COCHO), HCHO, CO, CO_2, CH_3COOH, CH_3OH, HCOOH and O_3 as identifiable products. The data have been analysed, utilising the results of a kinetic study of the oxidation of acetone in air. The mechanism of the oxidation proceeds initially *via* the production of acetonylperoxy radicals ($CH_3COCH_2O_2$) which are removed by their self-reaction (3), and reaction with other peroxy radicals [$CH_3C(O)O_2$, CH_3O_2 and HO_2] produced by the subsequent chemistry:

$$2CH_3COCH_2O_2 \rightarrow 2CH_3COCH_2O + O_2 \quad (3a)$$

$$\rightarrow CH_3COCHO + CH_3COCH_2OH + O_2 \quad (3b)$$

The thermal decomposition of CH_3COCH_2O radicals produced in channel (3a) into CH_3CO radicals and HCHO, is shown to predominate over the alternative reaction with O_2, under the conditions of these experiments:

$$CH_3COCH_2O + M \rightarrow CH_3CO + HCHO + M \quad (12)$$

$$CH_3COCH_2O + O_2 \rightarrow CH_3COCHO + HO_2 \quad (13)$$

Measurements of the yields of HCHO and CH_3COCHO are consistent with the operation of both channels of reaction (3) and allow certain conclusions to be drawn concerning the reactions of $CH_3COCH_2O_2$ with CH_3O_2 and $CH_3C(O)O_2$.

The only detected primary organic product of the oxidation of CH_3COCH_2OH is CH_3COCHO, formed with a yield of (100 ± 5)% by the following reaction sequence:

$$Cl + CH_3COCH_2OH \rightarrow HCl + CH_3COCHOH \quad (4)$$

$$CH_3COCHOH + O_2 \rightarrow CH_3COCHO + HO_2 \quad (5)$$

The concentration–time dependence of a range of secondary organic products, formed in the system was also measured. Identifiable products are CO, CO_2, CH_3COOH, HCHO, CH_3OH, HCOOH and pyruvic acid ($CH_3COCOOH$). These results are consistent with the presence of the $CH_3COCH(OH)O_2$ radical, formed as an intermediate in reaction (5):

$$CH_3COCH(OH)O_2 \leftrightarrow CH_3COCHO + HO_2 \quad (5'')$$

A knowledge of the detailed mechanisms by which organic compounds are degraded in the gas phase is necessary in order to assess their impact on the production of oxidants in the troposphere.[1,2] Organic peroxy radicals (RO_2) and the corresponding alkoxy radicals (RO), which are formed following the reaction of RO_2 with NO, are important intermediates in these reaction mechanisms, since several types of reaction are available for these species, particularly for the RO radicals.

The behaviour of RO under atmospheric conditions is dominated by three modes of reaction,[3–5] namely reaction with O_2, thermal decomposition or isomerisation. The relative importance of these three pathways has been investigated for a range of alkoxy radicals derived from simple alkanes, and rules for the prediction of the behaviour of related alkoxy radicals have been established.[6] In constrast, there have been far fewer studies of the behaviour of substituted alkoxy radicals[7–11] (*i.e.* those formed in the degradation of organic compounds other than alkanes), but it is becoming apparent that the rules applying to simple alkoxy radicals cannot be applied with confidence to the more complex, substituted counterparts.

The oxidation of acetone in the atmosphere may be initiated either by photolysis, or by reaction with OH radicals. The photolysis channels for acetone are well established[12–17] and, under tropospheric conditions, production of CH_3CO and CH_3 radicals appears to be the dominant process. Removal of acetone by reaction with OH radicals occurs approximately twice as quickly as photolysis to produce CH_3CO and CH_3,[17] but despite this, very little is known about the chemistry of the resultant acetonyl radical (CH_3COCH_2), which leads initially to the production of the acetonylperoxy radical:

$$OH + CH_3COCH_3 \rightarrow H_2O + CH_3COCH_2 \quad (1)$$

$$CH_3COCH_2 + O_2 \rightarrow CH_3COCH_2O_2 \quad (2)$$

We present the results of a product study of the oxidation of CH_3COCH_2 radicals formed from the reaction of Cl atoms and acetone, with product detection by long-path-length FTIR spectroscopy and long-path-length UV–VIS diode array spectroscopy. Although these experiments were performed in the absence of NO, production of the corresponding alkoxy radical occurs *via* one channel of the self-reaction of the peroxy radical:

$$2CH_3COCH_2O_2 \rightarrow 2CH_3COCH_2O + O_2 \quad (3a)$$

$$\rightarrow CH_3COCHO + CH_3COCH_2OH + O_2 \quad (3b)$$

In the following paper, a flash photolysis study of reactions of $CH_3COCH_2O_2$ is presented.[18] As a result of these studies, it is possible to draw some conclusions concerning the branching ratios of reaction (3), and of the reactions of $CH_3COCH_2O_2$ with other peroxy radicals produced in the system, and to establish the fate of the CH_3COCH_2O radical under atmospheric conditions.

Methyl glyoxal (CH_3COCHO) and hydroxyacetone (CH_3COCH_2OH) are expected to be major products of the oxidation of acetone, formed from reaction (3*b*). Recent studies have shown the rates of reaction of Cl atoms with CH_3COCHO and CH_3COCH_2OH to be greater than the rate of reaction of Cl atoms with acetone by approximately a factor of 20,[19–21] suggesting that they will compete for Cl atoms at relatively small fractional conversions of acetone, thereby influencing the observed product distribution. The mechanism of the Cl-atom-initiated oxidation of CH_3COCHO has been investigated.[20] In this paper, a study of the Cl-atom-initiated oxidation of CH_3COCH_2OH is presented. CH_3COCHO is the only detected primary organic product, and the mechanism of its *in situ* oxidation is explored.

Experimental

The majority of experiments were performed using the 'double multi-path' spectrometer at MPI, Mainz. This apparatus has been described in detail previously.[22] Briefly, it consists of a 44.2 l quartz reaction vessel equipped with two independent sets of White optics. This allows simultaneous monitoring of reagents and products using long-path-length FTIR spectroscopy, and long-path-length UV–VIS diode array spectroscopy. The reaction vessel is surrounded by seven sunlamps (Philips TL12/40W) emitting over the wavelength range 275–390 nm, enabling generation of Cl atoms by the photodissociation of Cl_2 in its near UV band. The photolysis of acetone was only of minor importance under the experimental conditions.

IR measurements were made in the range 400–4000 cm^{-1} using a Bomem DA03.01 FTIR spectrometer. UV–VIS measurements were made using a 60 W tungsten–halogen lamp with dispersion on a 0.5 m monochromator (B&M) and detection on an optical multichannel analyser (EG&G Model 1461) using a model 1412 silicon diode array detector, covering a range of 82 nm.

Reaction mixtures were typically made up of *ca.* 3×10^{15} molecule cm^{-3} Cl_2 (Linde, 1% in N_2) and *ca.* 2×10^{16} molecule cm^{-3} acetone (Aldrich, >99.9%), or *ca.* 10^{16} molecule cm^{-3} hydroxyacetone (Fluka, 99%). These were diluted with O_2 and N_2 (l'Air Liquide, High Purity). All experiments were performed at 298 K and at a total pressure of 700 Torr†.

A few supplementary experiments were carried out at Harwell using long-path-length UV–VIS diode array spectroscopy and the molecular modulation technique under similar conditions to those outlined above. Full details of this apparatus have been given previously.[23]

Results and Discussion

Photolysis of Cl_2 in the Presence of Hydroxyacetone and O_2

At short photolysis times, the Cl-atom-initiated oxidation of hydroxyacetone was found to yield methyl glyoxal as the only detected organic product, using long-path-length FTIR spectroscopy and long-path-length UV–VIS diode array spectroscopy. Its production is attributed to the following reaction sequence:

$$Cl + CH_3COCH_2OH \rightarrow HCl + CH_3COCHOH \quad (4)$$

$$CH_3COCHOH + O_2 \rightarrow CH_3COCHO + HO_2 \quad (5)$$

In order to provide further information, additional modulated photolysis experiments were performed on flowing gas mixtures (*i.e.* with residence times of *ca.* 10 s). This allowed time-resolved detection of HO_2 formed simultaneously with CH_3COCHO in reaction (5), by UV absorption spectroscopy at 220 nm, in the manner described before.[24] As shown in Fig. 1, the measured yield of HO_2 during the photolysis of Cl_2–CH_3COCH_2OH–O_2 mixtures was identical to that observed when CH_3COCH_2OH was substituted by H_2. In the latter case, quantitative conversion of Cl into HO_2 is well established.[24] Consequently, it is concluded that the Cl-atom-initiated oxidation of CH_3COCH_2OH generates HO_2 (and, by implication, CH_3COCHO) with a yield of (100 ± 5)% by reaction sequence (4) and (5). The observed time-dependence of HO_2 was consistent with its removal by the self-reaction to yield H_2O_2:

$$HO_2 + HO_2 \rightarrow H_2O_2 + O_2 \quad (6)$$

The attack of Cl exclusively at the $-CH_2OH$ group in CH_3COCH_2OH is consistent with the significantly greater reactivity of Cl atoms with CH_3COCH_2OH ($k_4 = 5.6 \times 10^{-11}$ cm^3 $molecule^{-1}$ s^{-1} [21]) than with acetone ($k = 2.4 \times 10^{-12}$ cm^3 $molecule^{-1}$ s^{-1} [19]), which suggests that a $-CH_2OH$ group adjacent to a carbonyl is some 40 times more reactive to Cl than a corresponding $-CH_3$ group. The subsequent formation of CH_3COCHO and HO_2 from reaction (5) is analogous to the observed formation of HO_2 and carbonyl compounds from the reactions of various α-hydroxyalkyl radicals with O_2.[25–29] Although a direct hydrogen-abstraction mechanism for these reactions may be important at higher temperatures,[25,26,29] the mechanism at ambient temperatures is believed to involve the formation of a peroxy radical intermediate which isomerises prior to decomposition to yield the observed products. Thus, for reac-

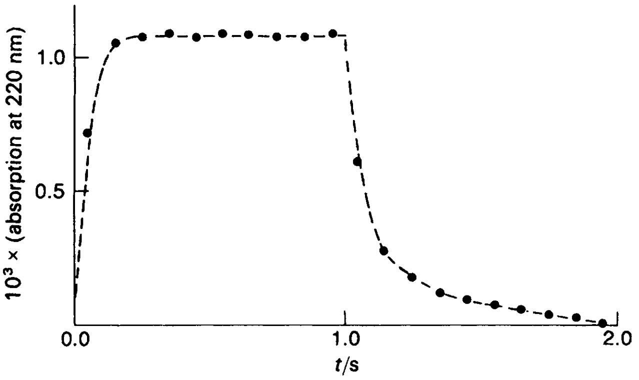

Fig. 1 HO_2 waveforms obtained during the Cl-atom-initiated oxidation of hydroxyacetone and H_2. (– – –) Cl_2–H_2–O_2 system, (●) Cl_2–hydroxyacetone–O_2 system.

---

† 1 Torr = (101 325/760) Pa.

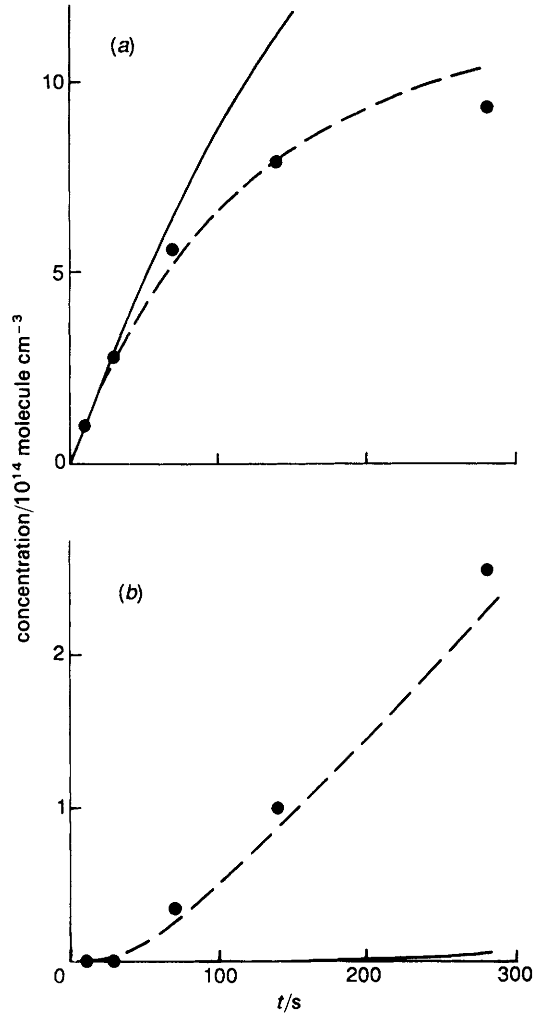

Fig. 2 Observed concentrations of (*a*) CH_3COCHO and (*b*) HCOOH, during the Cl-atom-initiated oxidation of hydroxyacetone. Lines represent calculated concentrations using the model in Table 1. Solid line assumes quantitative conversion of $CH_3COCH(OH)O_2$ to CH_3COCHO. Broken line allows for equilibrium (5″) and additional reactions of $CH_3COCH(OH)O_2$ (see text).

tion (5), the probable mechanism is as follows:

$$CH_3COCHOH + O_2 \rightarrow CH_3COCH(OH)O_2 \qquad (5')$$

$$CH_3COCH(OH)O_2 \leftrightarrow CH_3COCHO + HO_2 \qquad (5'')$$

Fig. 2 shows the time dependence of the accumulation of CH_3COCHO during the continuous photolysis of a static mixture of 3.6×10^{15} molecule cm^{-3} Cl_2 in the presence of 8.2×10^{15} molecule cm^{-3} CH_3COCH_2OH pressurised to 700 Torr with air. CH_3COCHO was measured primarily by differential diode array spectroscopy in the structured portion of its spectrum,[30] using the peak at 449.1 nm measured relative to a line constructed between the adjacent troughs at 448.5 and 449.8 nm. An initial linear build-up was observed, and this allowed calibration of the differential absorption cross-section [$\Delta\sigma(449.1 \text{ nm}) = 3.17 \times 10^{-20}$ cm^2 $molecule^{-1}$; 0.1 nm resolution] with the assumption that chlorine atoms produced CH_3COCHO quantitatively by the mechanism presented above. This cross-section was used to calibrate the yields of CH_3COCHO measured in the acetone oxidation experiments presented in the next section. The value of the cross-section is somewhat larger than expected from the spectrum of CH_3COCHO published by Plum *et al.*[31] In conjunction with the present study, the UV–VIS spectrum of CH_3COCHO has been characterised recently using the oxidation of CH_3COCH_2OH as a source.[30] Although the shape of the spectrum is in good agreement with that of Plum *et al.*, the absolute cross-sections are greater by about a factor of two.

Following the initial linear build-up of CH_3COCHO (Fig. 2), there is a rapid fall-off owing, in part, to the reaction of Cl atoms with CH_3COCHO competing with reaction (4):[20]

$$Cl + CH_3COCHO \rightarrow CH_3CO + CO + HCl \qquad (7)$$

FTIR spectroscopy allowed detection of a range of additional products formed from the secondary chemistry: CO, CH_3COOH, HCHO, CH_3OH, HCOOH, $CH_3COCOOH$ and CO_2. Green *et al.*[20] have studied the products of the Cl-atom-initiated oxidation of CH_3COCHO. On the basis of their results, the majority of these products might be rationalised in terms of the subsequent chemistry of CH_3CO [produced in reaction (7)] and HO_2 [produced in reaction (5)], as also shown in Fig. 3. However, the observed generation of HCOOH and $CH_3COCOOH$ requires an alternative explanation. This is particularly important for HCOOH which, apart from CO, was the major secondary product. The chemical system was simulated using FACSIMILE[32] and the chemical model listed in Table 1. In initial simulations, CH_3COCHO was removed solely by its reaction with Cl atoms [reaction (7)], the kinetics of which have been studied by Green *et al.*[20] ($k_7 = 4.8 \times 10^{-11}$ cm^3 $molecule^{-1}$ s^{-1}) and Wallington *et al.*[21] ($k_7 = 4.2 \times 10^{-11}$ cm^3 $molecule^{-1}$ s^{-1}). Fig. 2 shows a comparison of the calculated and observed

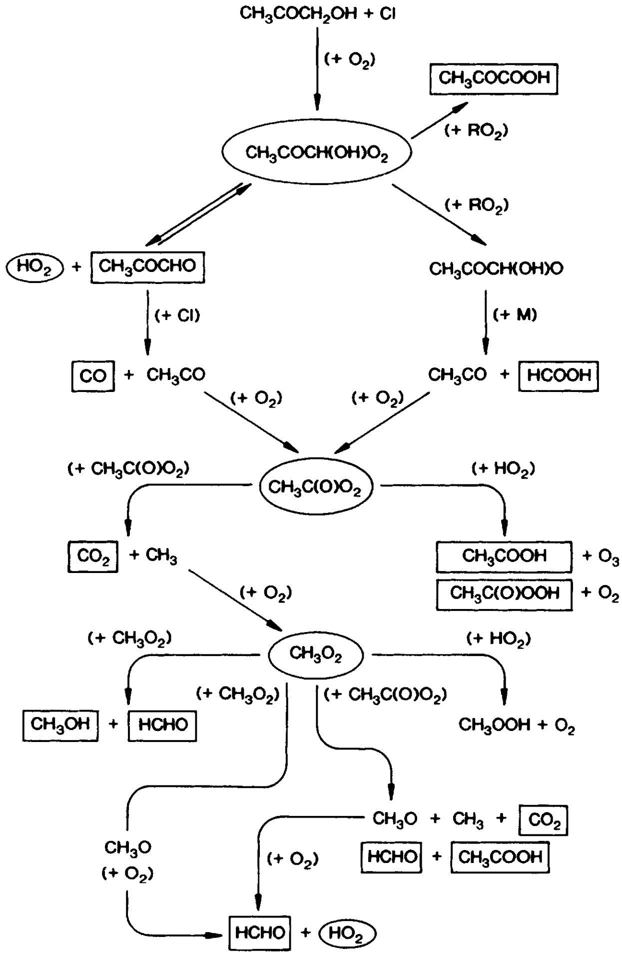

Fig. 3 Schematic representation of the Cl-atom-initiated oxidation of hydroxyacetone (RO_2 = unspecified peroxy radical). Boxed species are those observed during FTIR/diode array experiments.

Table 1 Chemical reactions and kinetic parameters used to simulate the Cl-atom initiated oxidation of acetone and hydroxyacetone

			rate constant[a]	ref.	comment
chlorine atom reactions					
(1)	$Cl + CH_3COCH_3$	$\rightarrow HCl + CH_3COCH_2$	2.4×10^{-12}	19	[b]
(4)	$Cl + CH_3COCH_2OH$	$\rightarrow HCl + CH_3COCHOH$	5.6×10^{-11}	21	
(7)	$Cl + CH_3COCHO$	$\rightarrow HCl + CH_3CO + CO$	4.5×10^{-11}	20, 21	[c]
	$Cl + HCHO$	$\rightarrow HCl + HCO$	7.3×10^{-11}	33	
	$Cl + CH_3OH$	$\rightarrow HCl + CH_2OH$	5.7×10^{-11}	33	
	$Cl + CH_3OOH$	$\rightarrow HCl + HCHO + OH$	5.7×10^{-11}	19	
	$Cl + CH_3COCH_2OOH$	$\rightarrow HCl + CH_3COCHO + OH$	1.0×10^{-10}	—	[b,d]
photolysis reactions					
	$Cl_2 + h\nu$	$\rightarrow Cl + Cl$	1.54×10^{-3}	—	[e]
	$CH_3COCH_3 + h\nu$	$\rightarrow CH_3CO + CH_3$	3.5×10^{-5}	—	[b,e]
	$CH_3COCHO + h\nu$	$\rightarrow CH_3CO + HCO$	1.9×10^{-4}	—	[e]
	$HCHO + h\nu$	$\rightarrow H_2 + CO$	7.1×10^{-5}	—	[e]
		$\rightarrow H + HCO$	3.5×10^{-5}	—	[e]
acetonylperoxy radical reactions					
(2)	$CH_3COCH_2 + O_2 + M$	$\rightarrow CH_3COCH_2O_2$	rapid	—	
(3*a*)	$CH_3COCH_2O_2 + CH_3COCH_2O_2$	$\rightarrow CH_3COCH_2O + CH_3COCH_2O + O_2$	6.0×10^{-12}	18	[b,c]
(3*b*)		$\rightarrow CH_3COCH_2OH + CH_3COCHO + O_2$	2.0×10^{-12}	18	[b,c]
(16*a*)	$CH_3COCH_2O_2 + CH_3C(O)O_2$	$\rightarrow CH_3 + CO_2 + CH_3COCH_2O + O_2$	5.0×10^{-12} (ratio varied)	18	[b,c]
(16*b*)		$\rightarrow CH_3COOH + CH_3COCHO + O_2$			
(15*a*)	$CH_3COCH_2O_2 + CH_3O_2$	$\rightarrow CH_3COCH_2O + CH_3O + O_2$	1.2×10^{-12}	18	[b,c]
(15*b*)		$\rightarrow CH_3COCH_2OH + HCHO + O_2$	2.6×10^{-12} (ratio varied)	18	[b,c]
(15*c*)		$\rightarrow CH_3COCHO + CH_3OH + O_2$			
	$CH_3COCH_2O_2 + HO_2$	$\rightarrow CH_3COCH_2OOH + O_2$	9.0×10^{-12}	18	[b,c]
acetylperoxy radical reactions					
	$CH_3CO + O_2 + M$	$\rightarrow CH_3C(O)O_2$	rapid		
	$CH_3C(O)O_2 + CH_3C(O)O_2$	$\rightarrow CH_3 + CH_3 + CO_2 + CO_2 + O_2$	1.6×10^{-11}	33	
	$CH_3C(O)O_2 + CH_3O_2$	$\rightarrow CH_3 + CO_2 + CH_3O + O_2$	5.5×10^{-12}	33	
		$\rightarrow CH_3COOH + HCHO + O_2$	5.5×10^{-12}	33	
(11*a*)	$CH_3C(O)O_2 + HO_2$	$\rightarrow CH_3COOH + O_3$	4.5×10^{-12}	34	[c]
(11*b*)		$\rightarrow CH_3COOOH + O_2$	8.5×10^{-12}	34	[c]
methylperoxy radical reactions					
	$CH_3 + O_2 + M$	$\rightarrow CH_3O_2$	rapid		
	$CH_3O_2 + CH_3O_2$	$\rightarrow CH_3O + CH_3O + O_2$	1.0×10^{-13}	33, 35	[f]
		$\rightarrow CH_3OH + HCHO + O_2$	2.4×10^{-13}	33, 35	[f]
		$\rightarrow CH_3OOCH_3 + O_2$	3.0×10^{-14}	33, 35	[f]
	$CH_3O_2 + HO_2$	$\rightarrow CH_3OOH + O_2$	4.8×10^{-12}	33	
formic acid formation ($HOCH_2O_2$ chemistry)					
(8)	$HO_2 + HCHO$	$\rightarrow HOCH_2O_2$	7.9×10^{-14}	33	
(-8)	$HOCH_2O_2$	$\rightarrow HO_2 + HCHO$	1.5×10^{2}	33	
	$HOCH_2O_2 + HOCH_2O_2$	$\rightarrow HOCH_2O + HOCH_2O + O_2$	5.2×10^{-12}	36	
		$\rightarrow HCOOH + HOCH_2OH + O_2$	7.0×10^{-13}	36	
	$HOCH_2O_2 + HO_2$	$\rightarrow HOCH_2OOH + O_2$	7.2×10^{-12}	36	
		$\rightarrow HCOOH + H_2O + O_2$	4.8×10^{-12}	36	
	$HOCH_2O_2 + CH_3O_2$	$\rightarrow HOCH_2O + CH_3O + O_2$	7.5×10^{-13}	—	[d]
		$\rightarrow HCOOH + CH_3OH + O_2$	3.8×10^{-13}	—	[d]
		$\rightarrow HOCH_2OH + HCHO + O_2$	3.8×10^{-13}	—	[d]
	$HOCH_2O_2 + CH_3C(O)O_2$	$\rightarrow HOCH_2O + CH_3 + CO_2 + O_2$	7.5×10^{-12}	—	[d]
		$\rightarrow HCOOH + CH_3COOH + O_2$	2.5×10^{-12}	—	[d]
	$HOCH_2O_2 + CH_3COCH_2O_2$	$\rightarrow HOCH_2O + CH_3COCH_2O + O_2$	4.4×10^{-12}	—	[b,d]
		$\rightarrow HCOOH + CH_3COCH_2OH + O_2$	1.1×10^{-12}	—	[b,d]
		$\rightarrow HOCH_2OH + CH_3COCHO + O_2$	1.1×10^{-12}	—	[b,d]
	$HOCH_2O + O_2$	$\rightarrow HCOOH + HO_2$	2.0×10^{-15}	—	[d]
formic acid formation ($CH_3COCH(OH)O_2$ chemistry)					
(5′)	$CH_3COCHOH + O_2 + M$	$\rightarrow CH_3COCH(OH)O_2 + M$	rapid		
(5″)	$CH_3COCH(OH)O_2$	$\rightarrow CH_3COCHO + HO_2$	varied		[c]
(-5″)	$CH_3COCHO + HO_2$	$\rightarrow CH_3COCH(OH)O_2$	varied		[c]
	$2CH_3COCH(OH)O_2$	$\rightarrow 2CH_3COCH(OH)O + O_2$	5.2×10^{-12}		[c]
		$\rightarrow CH_3COCOOH + CH_3COCH(OH)_2 + O_2$	7.0×10^{-13}		[c]
	$CH_3COCH(OH)O_2 + HO_2$	$\rightarrow$ products	1.2×10^{-11}		[c]
	$CH_3COCH(OH)O_2 + CH_3O_2$	$\rightarrow CH_3COCH(OH)O + CH_3O + O_2$	7.5×10^{-13}		[c]
		$\rightarrow CH_3COCOOH + CH_3OH + O_2$	3.8×10^{-13}		[c]
		$\rightarrow CH_3COCH(OH)_2 + HCHO + O_2$	3.8×10^{-13}		[c]
(9*a*)	$CH_3COCH(OH)O_2 + CH_3C(O)O_2$	$\rightarrow CH_3COCH(OH)O + CH_3 + CO_2 + O_2$	7.5×10^{-12}		[c]
(9*b*)		$\rightarrow CH_3COCOOH + CH_3COOH + O_2$	2.5×10^{-12}		[c]
(10)	$CH_3COCH(OH)O + M$	$\rightarrow HCOOH + CH_3CO + M$	rapid		

Table 1—*continued*

			rate constant[a]	ref.	comment
additional radical reactions					
(12)	$CH_3COCH_2O + M$	$\rightarrow CH_3CO + HCHO + M$	rapid		[b]
(14)	$CH_3O + O_2$	$\rightarrow HCHO + HO_2$	1.9×10^{-15}	33	
	$CH_2OH + O_2$	$\rightarrow HCHO + HO_2$	9.8×10^{-12}	33	
	$HCO + O_2$	$\rightarrow CO + HO_2$	5.6×10^{-12}	33	
	$HO_2 + HO_2$	$\rightarrow H_2O_2 + O_2$	2.8×10^{-12}	33	
	$OH + CH_3COCH_3$	$\rightarrow H_2O + CH_3COCH_2$	2.3×10^{-13}	33	[b]
	$OH + CO + O_2$	$\rightarrow CO_2 + HO_2$	2.3×10^{-13}	33	
	$OH + HCHO$	$\rightarrow H_2O + HCO$	1.1×10^{-11}	33	
	$OH + CH_3COCHO$	$\rightarrow H_2O + CH_3CO + CO$	1.7×10^{-11}	31	

[a] Units of rate constants: cm^3 $molecule^{-1}$ s^{-1} for bimolecular reactions, s^{-1} for unimolecular or photolysis reactions. [b] Reactions used in simulation of acetone system only. [c] See discussion in text. [d] Estimated by analogy. [e] Either measured in, or calculated for, experimental arrangement. [f] Overall value of rate constant taken from ref. (33), branching ratio taken from ref. (35).

time-dependence of CH_3COCHO, using a mean value of $k_7 = 4.5 \times 10^{-11}$ cm^3 $molecule^{-1}$ s^{-1}. The curvature in the concentration profile is seriously underestimated by the model, indicating that CH_3COCHO must either be removed by additional reactions in the system, or that its production is inhibited at longer photolysis times. Furthermore, the concentrations of the majority of the secondary products were underestimated, and additional conversion routes for CH_3COCHO into these products must exist.

As shown in Fig. 2, the concentrations of the major product HCOOH were underestimated by nearly two orders of magnitude. HCOOH was produced initially in the model only by the reactions of the $HOCH_2O_2$ radical formed from the well documented addition reaction of HO_2 and HCHO:[37]

$$HO_2 + HCHO \leftrightarrow HOCH_2O_2 \tag{8}$$

HCOOH has been shown to be produced from the reactions of $HOCH_2O_2$ with itself and HO_2.[36,38] Additional reactions with other peroxy radicals formed in the system [$CH_3C(O)O_2$ and CH_3O_2] were included, with rate coefficients estimated by analogy (see Table 1). As stated above, however, the observed concentrations of HCOOH were severely underestimated by the model. This is because HCHO was present only in low concentrations ($<10^{13}$ molecule cm^{-3} for the first 100 s photolysis), thereby precluding significant formation of $HOCH_2O_2$ by reaction (8).

The analogous equilibrium involving HO_2, CH_3COCHO and the hydroxyperoxy radical $CH_3COCH(OH)O_2$ was introduced above [reaction (5″)]. In the early stages of photolysis when CH_3COCHO concentrations are low, the back reaction producing $CH_3COCH(OH)O_2$ is precluded, and the peroxy radical is present only in low concentrations:

$$CH_3COCH(OH)O_2 \leftrightarrow CH_3COCHO + HO_2 \tag{5″}$$

As CH_3COCHO accumulates, however, the back reaction may be able to compete with removal of HO_2 by reaction (6), resulting in an increased concentration of $CH_3COCH(OH)O_2$. The possibility of alternative reactions for the peroxy radical must therefore be considered. In particular, the self-reaction and reactions with other peroxy radicals produced in the system at longer photolysis times [$CH_3C(O)O_2$ and CH_3O_2; see Fig. 3] are expected to be comparatively rapid resulting in the production of the alkoxy radical $CH_3COCH(OH)O$, which may decompose to produce HCOOH, *e.g.*:

$$CH_3COCH(O)HO_2 + CH_3C(O)O_2 \rightarrow$$
$$CH_3COCH(OH)O + CH_3 + CO_2 + O_2 \tag{9a}$$

$$CH_3COCH(OH)O + M \rightarrow CH_3CO + HCOOH + M \tag{10}$$

Additional calculations were performed, therefore, incorporating a speculative series of reactions for $CH_3COCH(OH)O_2$ with other peroxy radicals. Once again, the rate coefficients and branching ratios were estimated by analogy with known peroxy radical reactions (see Table 1). With these assumed values, an approximate estimate for the equilibrium constant for reaction (5″) of *ca.* 2×10^{15} molecule cm^{-3} was obtained by fitting to the experimentally observed CH_3COCHO profile (Fig. 2). As also shown in the figure, the observed production of HCOOH can be accounted for by this mechanism, with this equilibrium constant. Although the rates of the forward and reverse reactions cannot be determined independently from the present data, it was clear that $k_{5''}$ has to be greater than *ca.* 20 s^{-1} or else the self-reaction of $CH_3COCH(OH)O_2$ is competitive at short photolysis times and the production of CH_3COCHO is inhibited. Accordingly, the corresponding rate coefficient for the reverse reaction is $\geqslant 10^{-14}$ cm^3 $molecule^{-1}$ s^{-1}. This is somewhat greater than the single previous estimate of this rate coefficient, 2×10^{-15} cm^3 $molecule^{-1}$ s^{-1}.[39]

Further support for the generation of $CH_3COCH(OH)O_2$ in the system comes from the observation of bands due to $CH_3COCOOH$ in the product infrared spectra. This compound may be formed readily by reactions of the peroxy radical, *e.g.*:

$$CH_3COCH(OH)O_2 + CH_3C(O)O_2 \rightarrow$$
$$CH_3COCOOH + CH_3COOH + O_2 \tag{9b}$$

Note that another possible source of $CH_3COCOOH$ might arise in this system if the CH_3COCO species, formed as an intermediate in reaction (7), combined with O_2 to produce the peroxy radical $CH_3COC(O)O_2$. However, the available data of Green *et al.*[20] suggest that this cannot compete with thermal decomposition of CH_3COCO to yield CH_3CO and CO as shown above.

Photolysis of Cl_2 in the Presence of Acetone and O_2

The Cl-atom-initiated oxidation of acetone in the presence of O_2 resulted in the observation of CH_3COCHO, HCHO, CO, CO_2, CH_3COOH, CH_3OH, HCOOH and O_3 as identifiable products using both FTIR spectroscopy and UV–VIS diode array spectroscopy. CH_3COCH_2OH, however, was not positively identified. Its detection in the IR using the main absorption bands at *ca.* 1300 and 1750 cm^{-1} was precluded owing to other strongly absorbing species, and its other IR bands and its UV absorption spectrum are too weak for detection to be possible.

Experiments were typically performed with *ca.* $(1–2) \times 10^{16}$ molecule cm^{-3} of acetone. If less acetone was used, the concentrations of products such as CH_3COCHO and HCHO

Table 2 Equivalent carbon yields of products detected during the Cl atom-initiated oxidation of acetone

product	photolysis time/s 10	300
CH_3COCHO	0.222	0.116
HCHO	0.234	0.083
CO	0.024	0.186
CO_2	0.198	0.272
CH_3COOH	0.024	0.026
HCOOH	0.001	0.077
CH_3OH	0.033	0.026
total	0.736	0.786

were significantly suppressed owing to their rapid reactions with Cl atoms. If significantly more acetone was used, its removal by photolysis became competitive with removal by reaction with Cl atoms. Furthermore, portions of the IR spectrum became completely saturated at high acetone concentrations, inhibiting detection of certain products.

Equivalent carbon yields of all species detected relative to acetone lost by reaction with Cl atoms are shown in Table 2 for a typical experiment ($[Cl_2]_i = 3.45 \times 10^{15}$ molecule cm^{-3}; $[acetone]_i = 1.82 \times 10^{16}$ molecule cm^{-3}; $[O_2] = 2.0 \times 10^{19}$ molecule cm^{-3}). A simplified oxidation scheme describing production routes for some of the observed products is displayed in Fig. 4. Yields obtained after both 10 and 300 s photolysis are shown in the table. At the shorter reaction time (corresponding to *ca.* 0.5% conversion of acetone), HCHO, CH_3COCHO and CO_2 were the major products and *ca.* 74% of the acetone lost was accounted for by the measured products. The balance was almost certainly due to species such as CH_3COCH_2OH and various hydroperoxides which could not be detected. At the longer photolysis time corresponding to *ca.* 8% conversion of acetone), the product distribution observed was somewhat different. CO_2 and CO were the major products, and yields of HCHO and CH_3COCHO were significantly reduced compared with the shorter photolysis time, because they were removed by reaction with Cl atoms as they accumulated. This is also illustrated by the curvature in the concentration–time profiles for the species displayed in Fig. 5.

The production of the observed amounts of HCHO in the early stages of photolysis and some of the other products which are produced from the chemistry of CH_3CO, is indicative of the decomposition of the CH_3COCH_2O radical formed by the self reaction of $CH_3COCH_2O_2$ [reaction (3*a*)]:

$$2CH_3COCH_2O_2 \rightarrow 2CH_3COCH_2O + O_2 \qquad (3a)$$

$$\rightarrow CH_3COCHO + CH_3COCH_2OH + O_2 \qquad (3b)$$

$$CH_3COCH_2O + M \rightarrow CH_3CO + HCHO + M \qquad (12)$$

The potential alternative reaction of CH_3COCH_2O with O_2 would result in the production of CH_3COCHO as follows:

$$CH_3COCH_2O + O_2 \rightarrow CH_3COCHO + HO_2 \qquad (13)$$

In order to test whether reaction (13) was competing with reaction (12), similar experiments were performed for a range of $[O_2]$, and the influence on the observed products in general, and on CH_3COCHO and HCHO in particular, was investigated. Yields of CH_3COCHO and HCHO as a function of time, relative to acetone lost by reaction with Cl atoms, are displayed in Table 3 for three experiments with $[O_2] = 2.0 \times 10^{19}$, 4.9×10^{18} and 1.7×10^{17} molecule cm^{-3}.

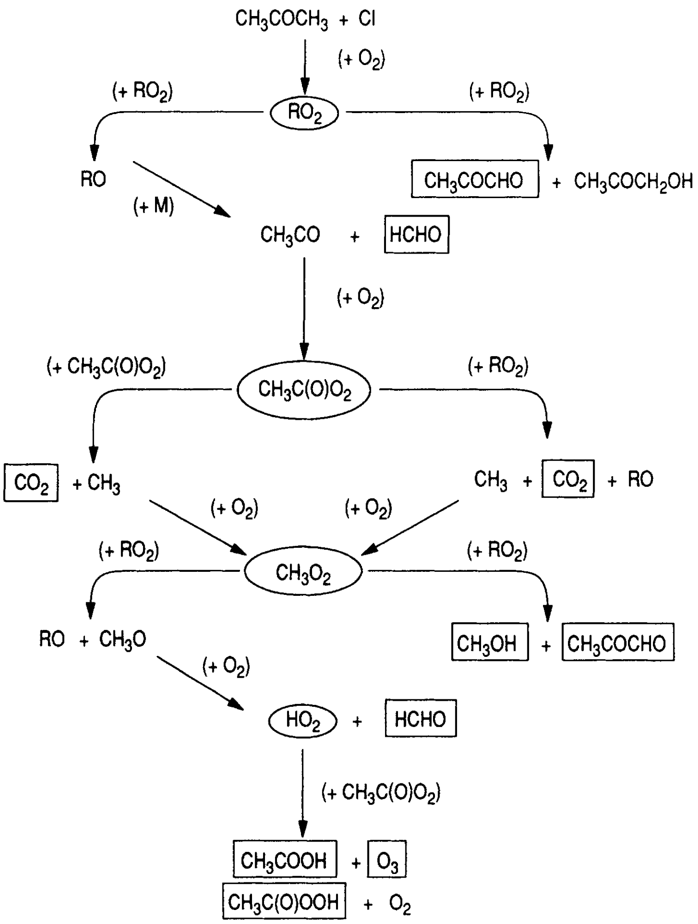

Fig. 4 Schematic representation of the Cl-atom-initiated oxidation of acetone ($RO_2 = CH_3COCH_2O_2$; $RO = CH_3COCH_2O$). Boxed species are those observed during experiments.

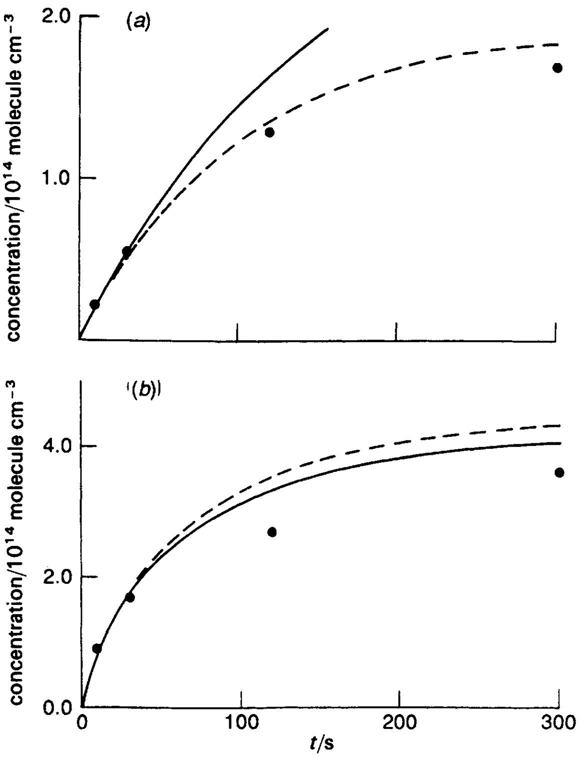

Fig. 5 Observed concentrations of (*a*) CH_3COCHO and (*b*) HCHO, during the Cl-atom-initiated oxidation of acetone. Lines represent calculated concentrations using the model in Table 1. Lines are best fits to 10 and 30 s data points. Broken line allows for equilibrium (5″) and additional reactions of $CH_3COCH(OH)O_2$.

Table 3 Yields of CH_3COCHO and HCHO as a function of photolysis time for various $[O_2]$

photolysis time/s	$[O_2]$/molecule cm^{-3}					
	2.0×10^{19}		4.9×10^{18}		1.7×10^{17}	
	CH_3COCHO	HCHO	CH_3COCHO	HCHO	CH_3COCHO	HCHO
10	0.222	0.234	—	—	0.201	0.224
30	0.202	0.168	0.198	0.174	0.198	0.179
120	0.153	0.116	0.159	0.119	0.161	0.115
300	0.116	0.083	0.125	0.074	0.118	0.075

It is apparent that the yields were insensitive to variation of O_2. This shows that reaction (13) was unable to compete with reaction (12), and that thermal decomposition of CH_3COCH_2O predominates under the conditions of these experiments. This agrees with the conclusions of the time-resolved experiments presented in the following paper.[18] The yields of the other observable products were also found to be insensitive to variation of $[O_2]$.

The reaction system was simulated using the chemical model shown in Table 1. The main aim of the modelling study was to describe accurately the production of the major products HCHO and CH_3COCHO during the early stages of photolysis before their removal by Cl atoms becomes significant. The production of these species is partitioned by the two channels of reaction (3). Reaction (3*a*) followed by reaction (12) produces HCHO, whereas (3*b*) produces CH_3COCHO directly. The observation of significant amounts of both products is a clear indication of the operation of both channels of reaction (3). There are, however, other sources of these products in the subsequent chemistry which need to be considered. Several other peroxy radicals [$CH_3C(O)O_2$, CH_3O_2 and HO_2] are produced rapidly in the reaction system (see Fig. 4), and their reactions with $CH_3COCH_2O_2$ will influence the partitioning between HCHO and CH_3COCHO. A kinetic study of the short-lived species produced in the Cl-atom-initiated oxidation of acetone, using the flash photolysis technique, is given in the following paper. The derived rate coefficients and branching ratios for reactions of $CH_3COCH_2O_2$ are used in the present simulations (see Table 1). Some additional measurements of peroxy radicals during the low intensity photolysis of Cl_2–acetone–O_2 mixtures have been made using the molecular modulation technique.[40] These experiments indicated that, at steady state, $CH_3COCH_2O_2$, $CH_3C(O)O_2$ and CH_3O_2 were present in comparable concentrations. In contrast, HO_2 is a minor radical in this system, since its production is essentially limited to the reaction of CH_3O with O_2 (see Fig. 4):

$$CH_3O + O_2 \rightarrow HCHO + HO_2 \qquad (14)$$

Accordingly, the present modelling study indicated that the initial production rates of HCHO and CH_3COCHO were sensitive to varying the branching ratios for the reactions of both CH_3O_2 and $CH_3C(O)O_2$ with $CH_3COCH_2O_2$. The reaction involving CH_3O_2 has three probable channels:

$$CH_3O_2 + CH_3COCH_2O_2 \rightarrow CH_3COCH_2O + CH_3O + O_2 \qquad (15a)$$

$$\rightarrow CH_3COCH_2OH + HCHO + O_2 \qquad (15b)$$

$$\rightarrow CH_3COCHO + CH_3OH + O_2 \qquad (15c)$$

These reactions partition HCHO and CH_3COCHO, since (15*a*) and (15*b*) produce HCHO either directly, or by the subsequent chemistry of CH_3COCH_2O [reaction (12)] and CH_3O [reaction (14)], whereas (15*c*) produces CH_3COCHO directly. The flash photoylsis experiments presented in the following paper established that (70 ± 10)% of the reaction proceeds *via* the terminating channels (15*b*) and (15*c*). In that study, however it was not possible to quantify the relative importance of the two channels, which influences the yields of HCHO and CH_3COCHO. The reaction of $CH_3C(O)O_2$ with $CH_3COCH_2O_2$ also has channels leading to the production of HCHO (16*a*) and CH_3COCHO (16*b*):

$$CH_3C(O)O_2 + CH_3COCH_2O_2$$

$$\rightarrow CH_3COCH_2O + CH_3 + CO_2 + O_2 \qquad (16a)$$

$$\rightarrow CH_3COCHO + CH_3COOH + O_2 \qquad (16b)$$

Although the overall rate coefficient for the reaction, k_{16}, was measured in the flash photolysis experiments, the branching ratio could not be established.

Modelling calculations were performed in which the contributions of reaction channels (15*b*) and (15*c*), and (16*a*) and (16*b*) were varied in order to influence the HCHO or CH_3COCHO producing potential of the reactions. Using a value of $(k_{15b} + k_{15c})/(k_{15a} + k_{15b} + k_{15c}) = 0.7$, in accordance with the results of the flash photolysis experiments, $k_{15b}/(k_{15a} + k_{15b} + k_{15c})$ $(=R_{15b})$ was fixed at various values in the range 0.0–0.7, and the branching ratio of reaction (16), $k_{16a}/(k_{16a} + k_{16b})$ $(=R_{16a})$, was optimised to achieve the best fit to the 10 and 30 s data points for HCHO and CH_3COCHO in each of the three experiments shown in Table 3. Mean fitted values for R_{16a} are listed in Table 4, and were found to vary in the range 0.00–0.77, depending on the value adopted for R_{15b}, indicating a strong anti-correlation between these parameters. However, it was clear that R_{15b} had to be <0.53 for reasonable fits to the data to be achieved. At greater values, too much HCHO was generated by the model, even if $R_{16a} = 0$. Computed concentration–time profiles for HCHO and CH_3COCHO are displayed in Fig. 5, with the experimental points for one experiment. The computed profiles correspond to $R_{15b} = 0.17$ and $R_{16a} = 0.47$, the parameter values for which the best fits to the data sets were obtained. On the basis of these calculations, we conclude the R_{15b} and R_{16a} lie in the ranges (0.2 ± 0.1) and (0.5 ± 0.2) respectively. Although the system was well described at short photolysis times, the model over-predicted

Table 4 Average optimised values of R_{16a} for various values of R_{15b}

R_{15b}	R_{16a}	
0.70	0.00[a]	(0.00)[a,b]
0.53	0.03	(0.00)
0.35	0.25	(0.19)
0.17	0.47	(0.42)
0.00	0.77	(0.72)

[a] Poor fits to data sets obtained. [b] Bracketted values are those obtained with equilibrium (5″) and additional reactions of $CH_3COCH(OH)O_2$ incorporated into the model (see discussion in text).

concentrations of both HCHO and CH_3COCHO at longer photolysis times. Incorporation of the equilibrium (5″) and additional reactions of $CH_3COCH(OH)O_2$, as discussed for the hydroxyacetone system, resulted in a significant improvement in the agreement between calculated and observed profiles at longer reaction times for CH_3COCHO, as shown in Fig. 5, although HCHO was still overestimated ($K^*_{5''} = 2 \times 10^{15}$ molecule cm^{-3}). Although not so sensitive to the change, the optimised fits to the data points for both HCHO and CH_3COCHO at short photolysis times were also marginally improved. The values of R_{16a} obtained are not significantly different however, and lie in the range 0.00–0.72 depending on the adopted value of R_{15b} as shown in Table 4.

The remainder of the observable products, CO, CO_2, CH_3COOH, CH_3OH, HCOOH and O_3 can all be accounted for by the reaction mechanism. The production of the major products at long photolysis times, CO and CO_2, was described adequately by the results of the modelling study. O_3 was a minor product, and the observed concentrations were consistent with its production from one channel of the $CH_3C(O)O_2 + HO_2$ reaction as observed previously:[34]

$$CH_3C(O)O_2 + HO_2 \rightarrow CH_3COOH + O_3 \quad (11a)$$

HCOOH is clearly generated as a secondary product in this system (see Table 2). As in the hydroxyacetone system, HCOOH was produced in the model initially by the reactions of $HOCH_2O_2$ formed from the addition reaction of HO_2 and HCHO [reaction (7)] which becomes increasingly important as HCHO accumulates. The known reactions of $HOCH_2O_2$ with HO_2 and itself, and the postulated reactions with $CH_3COCH_2O_2$, $CH_3C(O)O_2$ and CH_3O_2, which incorporate channels leading to the production of HCOOH, are listed in Table 1. Even with this additional chemistry, the model was unable to generate the observed concentrations of HCOOH. The analogous chemistry initiated by addition of HO_2 to CH_3COCHO as discussed above [equilibrium (5″)], although not as important in this system owing to the lower concentrations of HO_2 and CH_3COCHO, was able to increase the calculated HCOOH concentrations noticeably, but not sufficiently. However, since the model overpredicted the concentration of HCHO at longer photolysis times, (see Fig. 5), it seems likely that an additional conversion route for HCHO to HCOOH operates. If this is the case, then the observed concentrations of HCOOH, and those of HCHO at longer reaction times, can largely be explained. This may be a heterogeneous process occurring on reaction vessel walls at prolonged residence times.

Summary and Conclusions

Cl-atom-initiated Oxidation of CH_3COCH_2OH

The results presented indicate that CH_3COCHO is produced with a yield of (100 ± 5)% from the Cl-atom-initiated oxidation of CH_3COCH_2OH. This is attributed to the reaction sequence:

$$Cl + CH_3COCH_2OH \rightarrow HCl + CH_3COCHOH \quad (4)$$

$$CH_3COCHOH + O_2 \rightarrow CH_3COCHO + HO_2 \quad (5)$$

The observed curvature in the concentration–time profile for CH_3COCHO at longer photolysis times is explained partially by its removal by reaction with Cl atoms [reaction (7)] occurring in competition with reaction (4) as CH_3COCHO accumulates. However, the results are also consistent with the presence of the $CH_3COCH(OH)O_2$ radical in the system, formed as an intermediate in reaction (5):

$$CH_3COCH(OH)O_2 \leftrightarrow CH_3COCHO + HO_2 \quad (5'')$$

At longer photolysis times, the self reaction of $CH_3COCH(OH)O_2$ and reactions with other peroxy radicals produced in the system inhibits the production of CH_3COCHO by reaction (5″). The detection of $CH_3COCOOH$ and the observation of high concentrations of HCOOH provide further support for this explanation, since the former may be produced directly from reactions of $CH_3COCH(OH)O_2$, and the latter from the subsequent formation of $CH_3COCH(OH)O$ (see Fig. 3):

$$CH_3COCH(OH)O + M \rightarrow CH_3CO + HCOOH + M \quad (10)$$

Incorporation of the chemistry involving $CH_3COCH(OH)O_2$ into the modelling of the acetone oxidation experiments also resulted in a much improved agreement between predicted and observed concentrations of CH_3COCHO at longer photolysis times.

Cl-atom-initiated Oxidation of Acetone

The mechanism of the Cl-atom-initiated oxidation of acetone has been shown to be reasonably well represented by the reaction scheme listed in Table 1, incorporating rate coefficients and branching ratios for reactions of $CH_3COCH_2O_2$ presented in the following paper. The time-dependence of the major products, CH_3COCHO and HCHO, and some of the minor products, particularly in the early stages of photolysis, can be simulated accurately using this mechanism.

The chemistry of the system, and in particular the yields of CH_3COCHO and HCHO, was found to be insensitive to variation of $[O_2]$. This indicates that the observed CH_3COCHO was not generated significantly by the reaction of CH_3COCH_2O with O_2 [reaction (13)], but instead from the reactions of $CH_3COCH_2O_2$ with itself [reaction (3*b*)] and with CH_3O_2 [reaction (15*c*)] and $CH_3C(O)O_2$ [reaction (16*b*)]. The alternative channels for these reactions resulted in the production of HCHO [reactions (3*a*), (15*a*), (15*b*) and (16*a*)]. Certain conclusions can be drawn concerning these reaction channels:

(*a*) The observed yields of CH_3COCHO and HCHO can only be explained if reaction (3) has a significant contribution from both the non-terminating channel (3*a*) and the terminating channel (3*b*). This is consistent with the results of the flash photolysis experiments(18) from which $k_{3a}/(k_{3a} + k_{3b}) = 0.75$ was derived.

(*b*) The proportion of reaction (15) proceeding *via* the propagating channel (15*a*) was determined from the flash photolysis experiments, $k_{15a}/(k_{15a} + k_{15b} + k_{15c}) = 0.3$. The results from the present study suggest that both reaction channels (15*b*) and (15*c*) contribute to the reaction. The corresponding branching ratio (referred to earlier as R_{15b}) was determined simultaneously with R_{16a} allowing the following branching ratios to be defined:

$$CH_3O_2 + CH_3COCH_2O_2$$

$$\rightarrow CH_3COCH_2O + CH_3O + O_2 \quad (0.3 \pm 0.1) \quad (15a)$$

$$\rightarrow CH_3COCH_2OH + HCHO + O_2 \quad (0.2 \pm 0.1) \quad (15b)$$

$$\rightarrow CH_3COCHO + CH_3OH + O_2 \quad (0.5 \pm 0.1) \quad (15c)$$

$$CH_3C(O)O_2 + CH_3COCH_2O_2$$

$$\rightarrow CH_3COCH_2O + CH_3 + CO_2 + O_2 \quad (0.5 \pm 0.2) \quad (16a)$$

$$\rightarrow CH_3COOH + CH_3COCHO + O_2 \quad (0.5 \pm 0.2) \quad (16b)$$

It should be stressed that there is a strong anti-correlation between the calculated values of R_{15b} and R_{16a}. Ideally, further product studies are required in which CH_3O_2 and $CH_3C(O)O_2$ are produced as primary radicals (*i.e.* by addition of CH_4 or CH_3CHO to the reaction mixture) to allow these parameters to be determined independently.

The insensitivity of the CH_3COCHO and HCHO yields to $[O_2]$ establishes that the thermal decomposition of CH_3COCH_2O [reaction (12)] predominates over the reaction with O_2 [reaction (13)]. Modelling calculations suggest that if 10% of CH_3COCH_2O reacted with O_2 at the highest $[O_2]$ used ($= 2 \times 10^{19}$ molecule cm^{-3}), a trend in the observed yields of CH_3COCHO and HCHO with $[O_2]$ would have been discernible. Consequently, thermal decomposition occurs at least an order of magnitude more quickly than reaction with O_2 under these conditions. Reactions of alkoxy radicals with O_2 typically occur with a rate constant of *ca.* 8×10^{-15} cm^3 molecule^{-1} s^{-1}.[33] If this is assumed for CH_3COCH_2O, then thermal decomposition occurs at a rate of $k_{12} > 1.6 \times 10^6$ s^{-1}. This is entirely consistent with the estimate of Baldwin *et al.*[4] for α-carbonylalkoxy radicals in general (8.2×10^6 s^{-1}). This result also provides support for the thermal decomposition of $CH_3COCH(OH)O$ [reaction (10)] postulated to explain the production of HCOOH in the hydroxyacetone oxidation experiments.

Cox *et al.*[8] have shown that thermal decomposition also predominates for the α-carbonylalkoxy radical $CH_3CH(O)COCH_3$ formed in the oxidation of methyl ethyl ketone:

$$CH_3CH(O)COCH_3 + M \rightarrow CH_3CO + CH_3CHO + M \tag{16}$$

They were unable to detect biacetyl ($CH_3COCOCH_3$), which would be produced if the reaction with O_2 was significant. Furthermore, their study of the oxidation of methyl isobutyl ketone reported in the same paper indicated that the CH_3COCH_2O radical produced during the degradation decomposed to produce CH_3CO radicals, and subsequently peroxyacetyl nitrate (PAN). Importantly, no CH_3COCHO could be detected, establishing that reaction (13) was unable to compete with reaction (12) in their system, in agreement with the results of the present work. It seems reasonable to conclude, therefore, from the results of Cox *et al.*,[8] and from the results of the present studies, that α-carbonylalkoxy radicals in general will decompose to yield a carbonyl compound and an acyl radical under tropospheric conditions.

The authors gratefully acknowledge useful discussions with Tim Wallington (Ford Motor Company, Dearborn), Trudi Raber and John Crowley (both MPI Mainz), and the helpful comments of an anonymous reviewer concerning the hydroxyacetone oxidation mechanism. This work was carried out as part of the EUROTRAC project LACTOZ, and was funded partially by the Commission of the European Communities (contract EV4V-0082-C) and partially by the UK Department of the Environment (contract PECD 7/10/147).

References

1 R. Atkinson and A. C. Lloyd, *J. Phys. Chem. Ref. Data*, 1984, **13**, 315.
2 R. G. Derwent and M. E. Jenkin, *Atmos. Environ., Part A*, 1991, **25**, 1661.
3 K. R. Demerjian, J. A. Kerr and J. G. Calvert, *Adv. Environ. Sci. Technol.*, 1974, **4**, 1.
4 A. C. Baldwin, J. R. Barker, D. M. Golden and D. G. Hendry, *J. Phys. Chem.*, 1977, **81**, 2483.
5 L. Batt, *Int. J. Chem. Kinet.* 1979, **11**, 977.
6 W. L. Carter and R. Atkinson, *J. Atmos. Chem.*, 1985, **3**, 377.
7 H. Niki, P. D. Maker, C. M. Savage and L. P. Breitenbach, *Chem. Phys. Lett.*, 1981, **80**, 499.
8 R. A. Cox, K. F. Patrick and S. A. Chant, *Environ. Sci. Technol.*, 1981, **15**, 587.
9 R. A. Cox and A. Goldstone, *Proceedings of the 2nd European Symposium on the Physico-Chemical Behaviour of Atmospheric Pollutants*, Reidel, Dordrecht, 1982, pp. 112–119.
10 S. M. Japar, T. J. Wallington, J. F. O. Richert and J. C. Ball, *Int. J. Chem. Kinet.*, 1990, **22**, 1257.
11 T. J. Wallington and S. M. Japar, *Environ. Sci. Technol.*, 1991, **25**, 410.
12 W. A. Noyes, G. B. Porter and J. E. Jolley, *Chem. Rev.*, 1956, **56**, 49.
13 D. E. Hoare and G. S. Pearson, *Adv. Photochem.*, 1963, **3**, 83.
14 R. B. Cundall and A. S. Davies, *Prog. React. Kinet.*, 1967, **4**, 149.
15 E. K. C. Lee and R. S. Lewis, *Adv. Photochem.*, 1980, **12**, 1.
16 E. P. Gardner R. D. Wijayaratne and J. G. Calvert, *J. Phys. Chem.*, 1984, **88**, 5069.
17 H. Meyrahn, J. Pauly, W. Schneider and P. Warneck, *J. Atmos. Chem.*, 1986, **4**, 277.
18 I. Bridier, B. Veyret, R. Lesclaux and M. E. Jenkin, *J. Chem. Soc., Faraday Trans.*, 1993, **89**, 2993.
19 T. J. Wallington, J. M. Andino, J. C. Ball and S. M. Japar, *J. Atmos. Chem.*, 1990, **10**, 301.
20 M. Green, G. Yarwood and H. Niki, *Int. J. Chem. Kinet.*, 1990, **22**, 689.
21 T. J. Wallington, A. R. Potts and J. M. Andino, unpublished results.
22 G. K. Moortgat, R. A. Cox, G. Schuster, J. P. Burrows and G. S. Tyndall, *J. Chem. Soc., Faraday Trans. 2*, 1989, **85**, 809.
23 (*a*) R. A. Cox, and G. D. Hayman, *Nature* (*London*), 1988, **332**, 796; (*b*) M. E. Jenkin and R. A. Cox, *J. Phys. Chem.*, 1985, **89**, 192.
24 J. N. Crowley, F. G. Simon, J. P. Burrows, G. K. Moortgat, M. E. Jenkin and R. A. Cox, *J. Photochem. Photobiol. A*, 1991, **60**, 1.
25 H. H. Grotheer, G. Riekert, D. Walter and T. Just, *J. Phys. Chem.*, 1988, **92**, 4028.
26 F. L. Nesbitt, W. A. Payne and L. J. Stief, *J. Phys. Chem.*, 1988, **92**, 4030.
27 P. Pagsberg, J. Munk, C. Anastasi and V. J. Simpson, *J. Phys. Chem.*, 1989, **93**, 5162.
28 A. Miyoshi, H. Matsui and N. Washida, *Chem. Phys. Lett.*, 1989, **160**, 291.
29 A. Miyoshi, H. Matsui and N. Washida, *J. Phys. Chem.*, 1990, **94**, 3016.
30 R. Meller, J. N. Crowley, W. Raber, M. E. Jenkin and G. K. Moortgat, *J. Photochem. Photobiol. A*, 1991, **62**, 163.
31 C. N. Plum, E. Sanhueza, R. Atkinson, W. L. Carter and J. N. Pitts, *Environ. Sci. Technol.*, 1983, **17**, 479.
32 A. R. Curtis, and P. Sweetenham, *AERE Report R-12805*, 1987.
33 R. Atkinson, D. L. Baulch, R. A. Cox, J. R. Hampson, J. A. Kerr and J. Troe, *J. Phys. Chem. Ref. Data*, 1989, **18**, 881.
34 G. K. Moortgat, B. Veyret and R. Lesclaux, *Chem. Phys. Lett.*, 1989, **160**, 443.
35 O. Horie, J. N. Crowley and G. K. Moortgat, *J. Phys. Chem.*, 1990, **94**, 8198.
36 J. P. Burrows, G. K. Moortgat, G. S. Tyndall, R. A. Cox, M. E. Jenkin, G. D. Hayman and B. Veyret, *J. Phys. Chem.*, 1989, **93**, 2374.
37 F. Su, J. G. Calvert, J. H. Shaw, H. Niki, P. D. Maker, C. M. Savage and L. P. Breitenbach, *Chem. Phys. Lett.*, 1979, **65**, 221.
38 B. Veyret, R. Lesclaux, M. T. Rayez, J. C. Rayez, R. A. Cox and G. K. Moortgat, *J. Phys. Chem.*, 1989, **93**, 2368.
39 I. Barnes, K. H. Becker, E. H. Fink and F. Zabel, *3rd Discussion Meeting Working Party 2, CEC Cost 61A bis*, University College Dublin, 5–6th October 1982.
40 R. A. Cox and M. E. Jenkin, unpublished results.

Paper 2/06663G; *Received* 16*th December*, 1992